ejpmr, 2022, 9(7), 45-56

SJIF Impact Factor 6.222

EUROPEAN JOURNAL OF PHARMACEUTICAL AND MEDICAL RESEARCH

www.ejpmr.com

Research Article

ISSN 2394-3211

EJPMR

PROGRESSIVE EVALUATION OF CORTICAL HISTOMORPHOLOGY AND HISTOMORPHOMETRIC PARAMETERS IN ADULT WISTAR RATS FOLLOWING LITHIUM-PILOCARPINE-INDUCED TEMPORAL LOBE EPILEPSY

Sanmi Tunde Ogunsanya[1,4], Olugbenga Ayodeji Ayannuga[1], Adegbenga Rotimi Owolabi[2], Taiwo Olusola Osibogun[1,5] and Ayodeji Zabdiel Abijo[3]*

[1]Department of Anatomy and Cell Biology, Obafemi Awolowo University, Ile-Ife, Nigeria.
[2]Department of Medical Pharmacology and Therapeutics, Obafemi Awolowo University, Ile-Ife, Nigeria.
[3]Neurobiology Unit, Anatomy Department, Ben Carson (Snr) School of Medicine, Ilishan-Remo, Ogun State, Nigeria.
[4]Department of Anatomy, Ajayi Crowther University, Oyo, Oyo State.
[5]Department of Anatomy, Eko University of Medical and Health Sciences.

***Corresponding Author: Ayodeji Zabdiel Abijo**

Neurobiology Unit, Anatomy Department, Ben Carson (Snr) School of Medicine, Ilishan-Remo, Ogun State, Nigeria.

Article Received on 29/04/2022 **Article Revised on 20/05/2022** **Article Accepted on 10/06/2022**

ABSTRACT

Introduction: Temporal lobe epilepsy (TLE) the most common form of drug-refractory epilepsy in humans. This study evaluated the histomorphology of the neocortex, subcortical white matter and the timeline dynamics of the above parameters at different epileptogenesis phases following lithium-pilocarpine-induced TLE in Wistar rats. **Methods:** Sixty Wistar rats were assigned into 3 groups A-C (n=20each). A, B and C; acute, latent and chronic groups. Each group had 3 sub-groups {Control (5), sham (5) and experimental (10)}. Control and sham received 2mL/kg normal saline and diazepam (10mg/kg) intraperitoneally respectively. Experimental sub-group received lithium chloride (127mg/kg) subcutaneously 24hours prior pilocarpine administration. Pilocarpine (30mg/kg) was administered intraperitoneally. After seizure onset (90minutes), the experimental rats received diazepam (10mg/kg). The brains were excised and fixed in 10% neutral buffered formalin. Brain slices were obtained at the optic chiasm for routine paraffin embedding. Neuroarchitecture of the cortex was investigated using Hematoxylin and eosin (H&E) stains, while the morphology of white matter and the corpus callosum was demonstrated using Luxol fast blue. **Results:** Different layers of the cerebral cortex showed neurodegenerative characteristics in all three groups, with severe neurodegeneration in experimental sub-group compared to control and sham sub-groups. Subcortical white matter displayed non-compactness of the myelin sheath, resulting in greater white matter thickness in the experimental sub-groups compared to the compact myelin sheath found in control and sham. **Conclusion:** Conclusively, progressive neurodegeneration observed in the cerebral cortex as well as the demylineation dynamics seen in subcortical white matter further explains the scientific basis of epileptogenesis following lithium-pilocarpine-induced TLE.

KEYWORDS: TLE, lithium-pilocarpine, epileptogenesis, demyelination.

1.0 INTRODUCTION

Epilepsy is characterized by recurrent unprovoked epileptic seizures caused by abnormal discharges of electrical activity in the brain cells which may lead to abnormal behavioral patterns (Fisher *et al.*, 2005). It affects an estimated 1% of the world's population and has no respect for age and gender (Moshi *et al.*, 2005). Temporal lobe epilepsy (TLE) is the most common form of epilepsy in humans (Bertram, 2009). In TLE, seizures spread to neighboring cortices and there is hippocampal neuronal loss (Kandratavicius *et al.*, 2013). It is one of the most common forms of drug-refractory epilepsy (Duncan *et al.*, 2006). Affected patients often have similar clinical history, including an initial precipitating injury such as febrile convulsions, status epilepticus (SE), or trauma (Rigoulot *et al.*, 2004). Between this injury and the emergence of recurrent complex partial seizures, there is usually a latent period of several years. Frequently associated with this epilepsy is the presence of hippocampal sclerosis (Jutila *et al.*, 2001). The lithium-pilocarpine model of TLE in rats is one of the most commonly used experimental models of epilepsy that reproduces most of the clinical and neuropathological features of human TLE (Turski *et al.*, 1983; Pitkänen *et al.*, 2006). TLE is the most common drug-resistant epilepsy in adults. Although hippocampal atrophy is the distinguishing characteristic of this disorder (Cascino *et al.*, 1991). Abundant magnetic resonance imaging (MRI)-based analyses of gray matter including volumetry, voxel-based morphometry, and

cortical thickness measurement have shown that structural changes extend to temporolimbic and frontocentral regions (Bernasconi *et al.*, 2003; Bernhardt *et al.*, 2008; Keller and Roberts, 2008). Several studies have also highlighted marked morphological (Bernasconi *et al*. 2004; McMillan *et al.*, 2004; Seidenberg *et al.*, 2005) and microstructural (Concha *et al.*, 2005; Yogarajah and Duncan 2008) white matter abnormalities located within and beyond the temporal lobes. Aside from static changes, there is recent evidence that atrophy intensifies over time, likely as a result of seizure-induced damage (Theodore and Gaillard, 2002; Sutula *et al.*, 2003; Bernhardt *et al.*, 2009; Cascino, 2009; Coan *et al.*, 2009).

2.0 Chemicals and Drugs

Lithium chloride was procured from Sigma-Aldrich (USA). Pilocarpine hydrochloride was purchased from Sigma-Aldrich (USA). Diazepam was procured from F. Hoffmann-La Roche Ltd, Basel (Switzerland). Other reagents used were of analytical grade.

2.1 Rat Care and Management

Sixty 12 weeks old adult Wistar rats were utilized for this study. The rats were bred at the Animal Holding of the Department of Anatomy and Cell Biology where they were housed in plastic cages. The animal room was kept under standard laboratory conditions of temperature, humidity, and light. Rats were fed on standard laboratory rat chow (ACE feed, Osogbo, South-West Nigeria, West Africa) and had access to water *ad libitum*. Ethical clearance was obtained from the Health Research and Ethics Committee (HREC) of the Institute of Public Health, Obafemi Awolowo University, Ile-Ife. The rats received humane care according to the guidelines for the use of animals documented by the National Research Council of Thailand, 1999.

2.2 Experimental design

Rats in group A were the acute group, rats in group B were the Latent group and rats in group C were the chronic group. Rats in each group were subdivided into 5 control, 5 sham control and 10 experimental sub-groups. Control rats in all groups received normal saline intraperitoneally, which served as vehicle for the administration of pilocarpine and lithium chloride. Sham control rats in all groups received normal saline intraperitoneally, and were also administered diazepam at a dose of 10 mg/kg body weight intraperitoneally which is equivalent to the dose administered to the experimental rats. Experimental rats were administered lithium chloride at a dose of 3 mEq/kg (127 mg/kg) body weight subcutaneously 24 hours prior to administration of pilocarpine. Pilocarpine was administered at a dose of 30 mg/kg body weight intraperitoneally to the experimental rats. Following 90 minutes of acute seizure (Status Epilepticus) onset, the experimental rats received diazepam injection at a dose of 10 mg/kg body weight intraperitoneally.

Table 1: **Summary of Experimental Design and Grouping.**

Groups (n= 20 each)	Subgroups	Intervention	Dose Regimen
Acute (Group A)	Control (n= 5)	Normal Saline	2 mLs/kg
	sham (n= 5)	Diazepam	10 mg/kg
	Experimental (n= 10)	Lithium chloride Pilocarpine	3mEq/kg (127 mg/kg) 30 mg/kg
Latent (Group B)	Control (n= 5)	Normal Saline	2 mLs/kg
	Sham (n= 5)	Diazepam	10 mg/kg
	Experimental (n= 10)	Lithium chloride Pilocarpine	3mEq/kg (127 mg/kg) 30 mg/kg
Chronic (Group C)	Control (n= 5)	Normal Saline	2 mLs/kg
	Sham (n= 5)	Diazepam	10 mg/kg
	Experimental (n= 10)	Lithium chloride Pilocarpine	3mEq/kg (127 mg/kg) 30 mg/kg

2.3 Determination of Body Weight and Brain Weight

The weight of the rats was taken using a top loader balance. Bodyweight was expressed as the percentage difference between the final and initial body weights divided by initial weight.

$$\text{Weight change} = \frac{\text{final weight} - \text{initial weight (g)}}{\text{Initial weight}}$$

Brain weights were taken on a top loader digital balance at sacrifice. Relative brain weight was defined as the percentage ratio of liver weight to final body weight.

$$\text{Relative brain weight} = \frac{\text{Brain weight x 100\%}}{\text{Final body weight}}$$

2.4 Animal Sacrifice
Rats were sacrificed under Ketamine anesthesia (90 mg/kg i.m). The skulls were opened carefully to avoid brain tissue damage. The brains were excised and fixed in 10% Neutral Buffered Formalin (NBF). One mm thick coronal brain slice was obtained at the level of the optic chiasma and processed for routine paraffin embedding.

2.5 Histological Procedure
The tissues were kept in this fixative at room temperature till they were processed. Tissues were processed via the paraffin wax embedding method (Drury and Wallington 1980). Sections of 5µm thickness were obtained on a rotary microtome (Leica RM 2125 RTS) and were stained with Hematoxylin and Eosin for the demonstration of general neuroarchitecture for evaluation of necrotic changes and Luxol fast blue for demonstration of subcortical white matter and corpus callosum.

2.5.1 Photomicrography
Brain sections were examined under a LEICA research microscope (DM750) connected to a digital camera (LEICA ICC50) and permanent photomicrographs were taken. Scale bars were merged on each micrograph taken.

2.5.2 Image Analysis
Integrated morphology analysis was undertaken using Image J software. Digital images were uploaded unto the image J analysis software and scale was set using a digital micrometer gauge reading to convert measurements in pixels to microns and this was applied globally to all images. Cells were counted using the cell counter plug-in available on the Image J analysis software after a grid had been superimposed on the photomicrograph.

2.6 Histological Scoring
Quantification of neuronal degeneration and normal neurons were carried out as follows: the number of degenerated neurons and normal neurons was counted in 7 high power fields (400x) of Hematoxylin and Eosin stained sections taking account of the following morphological criteria: increased eosinophilia with or without shrunken nuclei, cell swelling and lysis, intracytoplasmic vacuolation, Neuronal vacuolation, pyknosis, karyolysis, and karyorrhexis in the upper and lower cortical regions (Carliss *et al.*, 2007; Garman, 2011).

2.6 Statistical Analysis
Data were analyzed using t-test for comparison between two sub-groups. GraphPad Prism 5 (Version 5.03, GraphPad Inc.) was the statistical package used for data analysis. Significant difference was set at $p<0.05$.

3.0 RESULTS
3.1 Effect of seizure on brain weight, relative brain weight, and body weight
In the acute group, the study showed no significant difference in brain weight when the experimental sub-group was compared with control (p=0.3201) and sham control (p=0.8726) sub-groups. The latent group showed no significant difference in brain weight when the experimental sub-group was compared to control (p=0.6609) and sham control (p=1.0000) sub-groups. In the chronic group, the study showed a significant difference in brain weight when the experimental sub-group was compared with the control sub-group (p=0.0024).

Table 2: Brain Weight and Relative Brain Weight of Acute, Latent and Chronic Groups.

	Brain Weight (g)	Relative Brain Weight (%)
Acute control	1.69±0.01	1.23±0.04
Acute sham	1.74±0.03	1.24±0.04
Acute experimental	1.75±0.04	1.26±0.03
Latent control	1.76±0.05	1.22±0.02
Latent sham	1.74±0.02	1.22±0.05
Latent experimental	1.74±0.02	1.28±0.02
Chronic control	1.71±0.01	1.06±0.05
Chronic sham	1.76±0.02	1.12±0.02
Chronic experimental	1.77±0.01*	1.11±0.02

*- Significant difference when chronic experimental sub-group was compared with chronic control sub-group ($p<0.05$). Values are expressed as mean±SEM.

3.1.1 Weight Change in Acute Group
The study showed a significant decrease in body weight gained when the experimental sub-group was compared with control (p<0.0001) and sham (p<0.0001) sub-groups during the acute phase.

3.1.2 Weight Change in Latent Group
In this study, there is a significant reduction in body weight when the experimental sub-group was compared with the control (p<0.0001) and sham (p<0.0001) sub-groups but no significant difference was observed when control was compared with sham control (p=0.8396) during the acute phase. In the latent phase, the

experimental sub-group showed a significant decrease in weight gained when the experimental sub-group was compared with the control ($p<0.0001$) and sham ($p<0.0001$) sub-groups.

3.1.3 Weight Change in Chronic Group

The study showed a significant reduction in body weight when the experimental sub-group was compared with control ($p<0.0001$) and sham ($p<0.0001$) sub-groups. In the latent phase, the experimental sub-group showed a significant decrease in weight gained when compared with both control ($p<0.0001$) and sham ($p<0.0001$). In the chronic phase, the experimental sub-group showed a significant decrease in weight gained when compared with control ($p=0.0005$) and sham ($p=0.0045$) sub-groups.

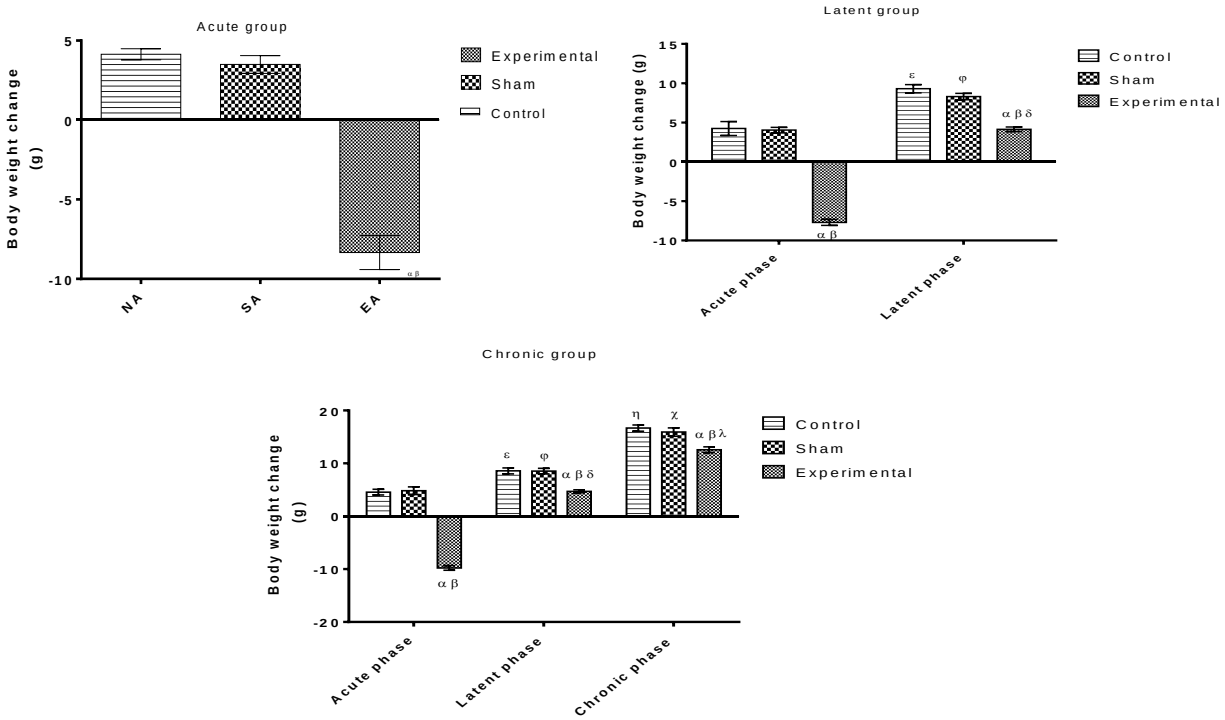

Figure 3.1: Graphs showing body weight change in acute, latent, and chronic groups. *α*, β – significant difference between experimental when compared with control and sham sub-groups respectively. ε, φ and δ - significant difference between (acute) control, sham, and experimental sub-groups when compared with (latent) control, sham, and experimental sub-groups respectively ($p<0.05$). η, χ and λ– significant difference between (acute) control, sham and experimental sub-groups when compared with (chronic) control, sham and experimental sub-groups respectively Values are expressed as mean ± SEM

Haematoxylin and Eosin (H&E) Staining Results

4.4.1 Cortical Histology and Histomorphometric analysis

These results revealed that the acute group showed a significant decrease in the number of normal neuronal density present in the experimental sub-group when compared with control ($p=0.0006$) and sham sub-groups ($p<0.0001$) but no significant difference was observed when control was compared with sham control ($p=0.7742$) of the dorsolateral cerebral cortex. However, degenerating neuronal density significantly increased in the experimental sub-group when compared with control ($p<0.0001$) and sham ($p<0.0001$) sub-groups but no significant difference was observed when control was compared with sham control ($p=0.1051$).

In the latent group, the number of neurons showing degenerating features was significantly more in the experimental sub-group when compared with control ($p<0.0001$) and sham ($p<0.0001$) sub-groups but no significant difference was observed when control was compared with sham control ($p=0.6232$). Correspondingly, the number of normal neurons was significantly decreased in the experimental sub-group when compared with control ($p<0.0001$) and sham ($p<0.0001$). Also, no significant difference was observed when control was compared with sham control ($p=0.6677$).

In the chronic group, the number of neuronal density showing degenerating features was significantly more in the experimental sub-group when compared with control ($p<0.0001$) and sham ($p<0.0001$) sub-groups but no significant difference was observed when control was compared with sham control ($p=0.5705$). Correspondingly, the number of normal neuronal density was significantly decreased in the experimental sub-group when compared with control ($p=0.0006$) and sham ($p<0.0001$) sub-groups but no significant difference was observed when control was compared with sham control

(p=0.2399). These results revealed a significant increase in degenerating neurons of the dorsolateral cortex when the experimental sub-group of the acute group was compared with the experimental chronic (p=0.0011) sub-group. Also, there was a significant difference when the experimental sub-group of the latent group was compared with the experimental sub-group of the chronic group (p=0.0234). However, no there was a significant difference when the experimental subgroup of the latent group was compared with the experimental sub-group of the acute group (p=0.0741).

These results revealed that the acute group showed a significant increase in oligodendrocyte density when the experimental sub-group was compared with control (p=0.0003) and sham (p<0.0001) sub-groups but no significant difference was observed when control was compared with sham control (p=0.2322). The latent group also showed a significant increase when experimental sub-group was compared with control (p<0.0001) and sham (p<0.0001) sub-groups but no significant difference was observed when control was compared with sham control (p=0.6236). In the chronic group, oligodendrocyte density was significantly more when the experimental sub-group was compared with control (p=0.0247) and sham (p=0.0002) sub-groups but no significant difference was observed when control was compared with sham control (p=0.9878).

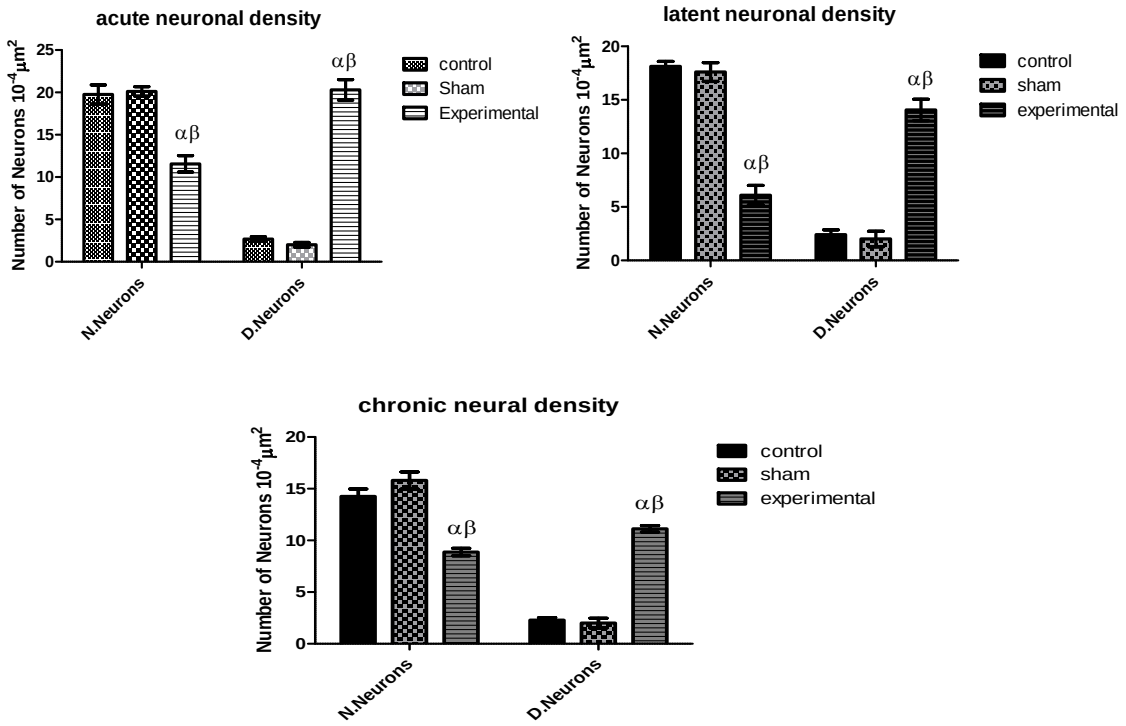

Figure 3.2: Charts represent the neuronal density of upper and lower cortical regions of acute, latent, and chronic groups. α, β – represents significant difference when the experimental sub-group is compared with control and sham control sub-groups respectively (p<0.05). N. Neurons – Normal Neurons, D. Neurons – Neurons showing degenerating features. Values are expressed as mean ± SEM

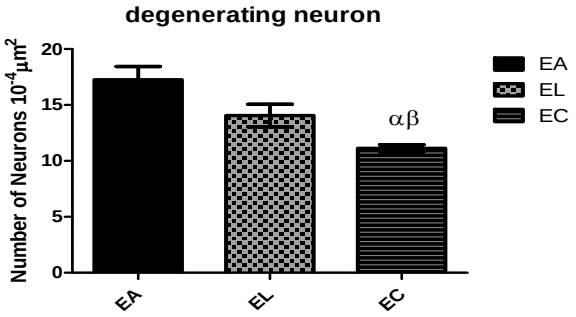

Figure 3.3: Bar chart showing neuronal degeneration of upper and lower cortical regions across the experimental sub-groups. α– significant difference when acute experimental sub-group is compared with chronic experimental sub-group; β- significant difference when latent experimental sub-group is compared with chronic

experimental sub-group; D. Neurons – Neurons showing degenerating features; EA- Acute experimental sub-group; EL- Latent experimental sub-group; EC- chronic experimental sub-group.Values are expressed as mean±SEM. Statistical significance at (p<0.05).

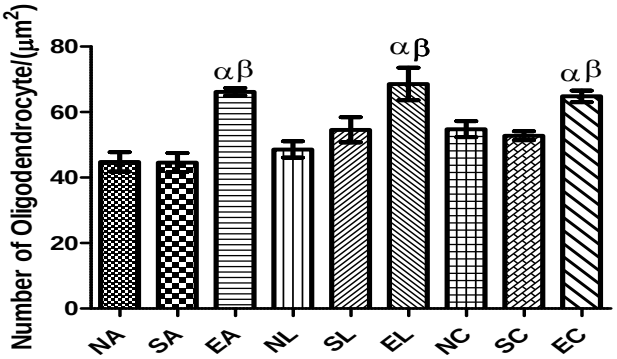

Figure 3.4: Bar chart showing oligodendrocyte density of H&E stained sections of upper and lower cortical regions. α, β – significant difference when experimental sub-group is compared with control and sham control sub-groups respectively. NA- Acute control sub-group; SA- Acute sham control sub-group; EA- Acute experimental sub-group; NL- Latent control sub-group; SL- Latent sham control sub-group; EL- Latent experimental sub-group NC- Chronic control sub-group; SC- Chronic sham control sub-group; EC- chronic experimental sub-group. Values are expressed as mean±SEM.

Histopathological evaluation

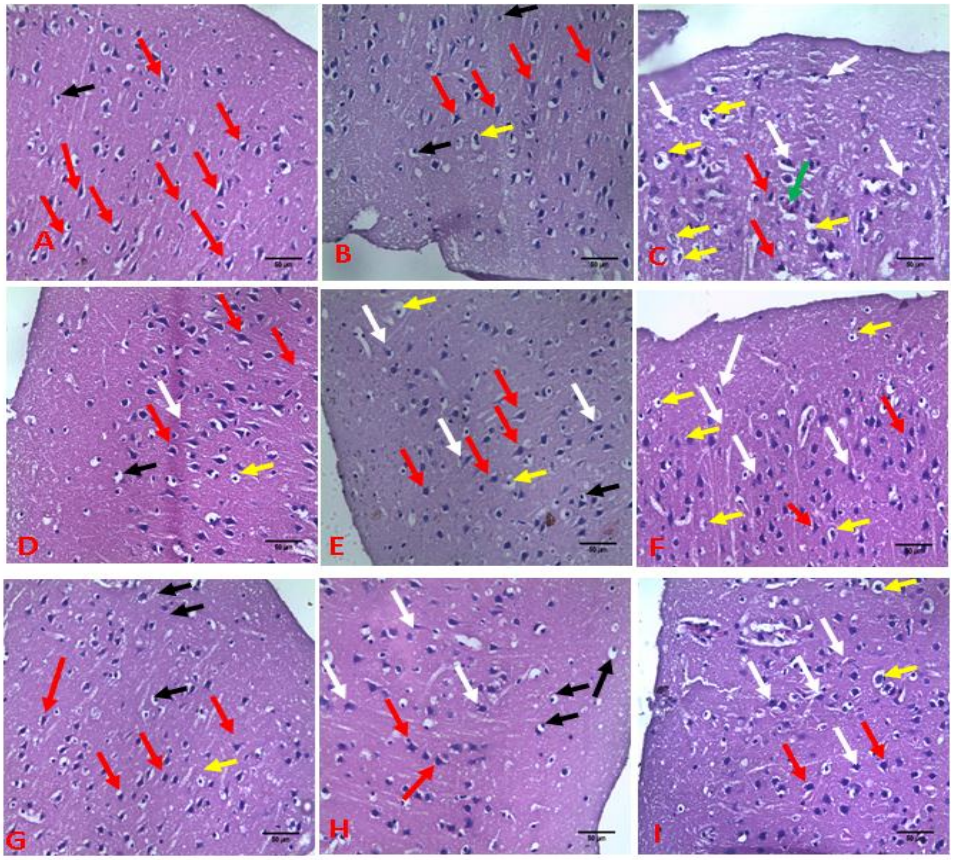

Plate 3.1: Representative light Photomicrographs of the upper cortical region (consisting of cortical layers I and II) subjected to H&E stain. The upper panel represents acute sub-groups (Control, sham, and experimental {A, B, and C} respectively). The middle panel represents latent sub-groups (Control, sham, and experimental {D, E, and F} respectively). The lower panel represents chronic sub-groups (Control, sham, and experimental {G, H, and I} respectively). White arrow-pyknotic neurons, Green arrow-eosinophilic neuron, Yellow arrow-Vacuolated neuron, Red arrow – intact neuron, Black arrow – oligodendrocytes. Scale bars- 50μm

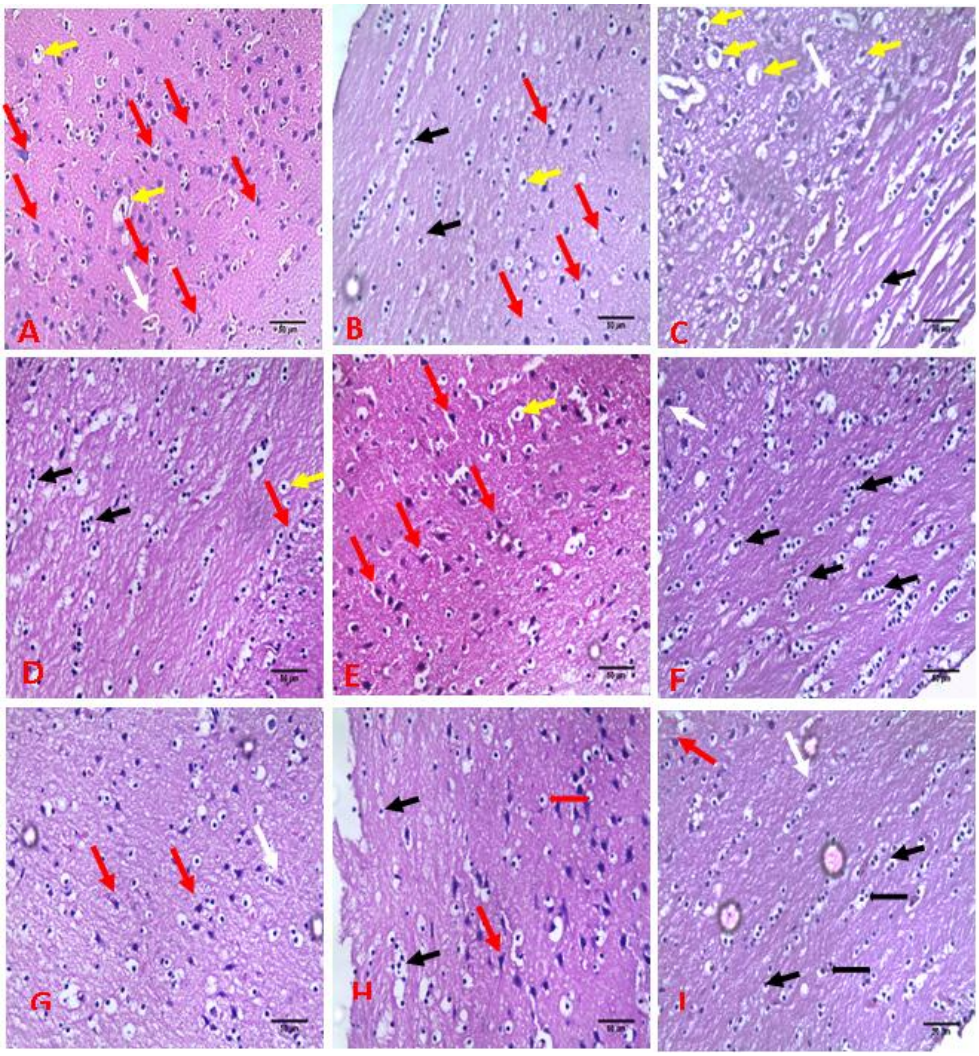

Plate 3.2: Representative light photomicrographs of the lower cortical region (consisting of cortical layers V and VI) subjected to H&E stain. The upper panel represents acute sub-groups (Control, sham, and experimental {A, B, and C} respectively). The middle panel represents latent sub-groups (Control, sham, and experimental {D, E, and F} respectively). The lower panel represents chronic sub-groups (Control, sham and experimental {G, H and I} respectively). White arrow- pyknotic neuron, Yellow arrow- vacuolated neuron, Red arrow – intact neuron, Black arrow – oligodendrocytes. Scale bars- 50μm.

3.2 Luxol Fast Blue (LFB) Staining Results

3.2.1 Histomorphometric analysis of the subcortical white matter and corpus callosum

Sections were measured for thickness of the subcortical white matter which is predominantly filled with myelin sheath and also thickness of the corpus callosum. The CA2 region of the hippocampus served as the landmark for the measurement of subcortical thickness.

Using the Image J software, subcortical white matter and corpus callosum thicknesses were evaluated.

These results revealed that the acute group showed a significant increase in thickness of the subcortical white matter when the experimental sub-group was compared with control ($p=0.0003$) and sham ($p<0.0001$) sub-groups. The latent group also showed a significant increase in thickness when the experimental sub-group was compared with control ($p<0.0001$) and sham ($p<0.0001$) sub-groups. In the chronic group, the thickness of the subcortical white matter was significantly more when the experimental sub-group was compared with control ($p=0.0247$) and sham ($p=0.0002$) sub-groups.

These results revealed that the acute group showed a significant increase in thickness of the corpus callosum when the experimental sub-group was compared with control ($p=0.0025$) and sham ($p=0.0049$) sub-groups. The latent group showed no significant difference in thickness when the experimental sub-group was compared with control ($p=0.1703$) and sham ($p=0.0996$) sub-groups. In the chronic group, the thickness of the corpus callosum was significantly more when the experimental sub-group was compared with control ($p=0.0151$) and sham ($p=0.0077$).

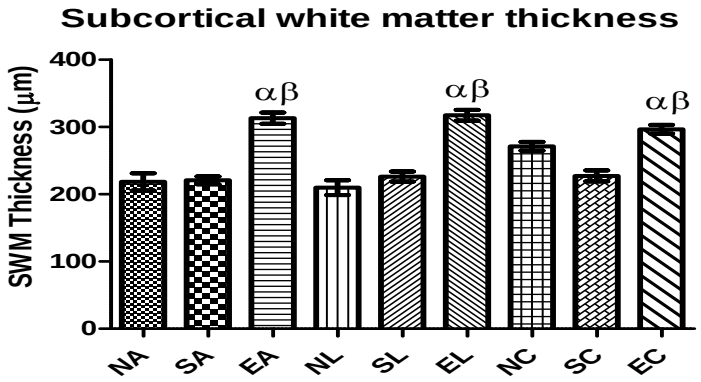

Figure 3.5: Bar chart showing measurement of thickness of the subcortical white matter. α, β – significant difference when experimental is compared with control and sham of the same sub-group respectively. NA – Acute control; SA – Acute sham; EA – Acute Experimental; NL – Latent control; SL- Latent sham; EL- Latent experimental; NC- Chronic control; SC; Chronic sham; EC- Chronic experimental. Values are expressed as mean±SEM

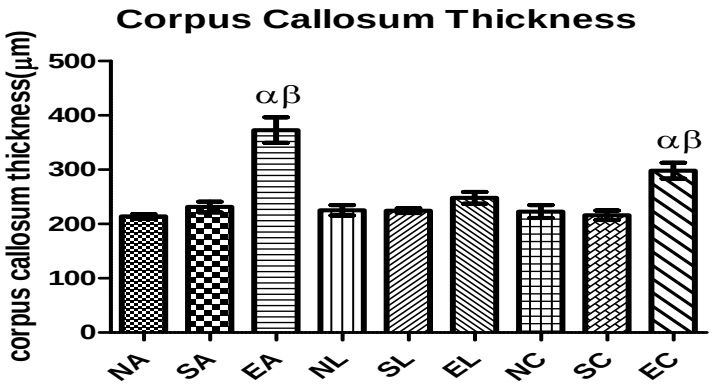

Figure 3.6: Bar chart showing measurement of the thickness of the corpus callosum. α, β – significant difference when experimental is compared with control and sham of the same sub-group respectively. NA – Acute control; SA – Acute sham; EA – Acute Experimental; NL – Latent control; SL- Latent sham; EL- Latent experimental; NC- Chronic control; SC; Chronic sham; EC- Chronic experimental. Values are expressed as mean±SEM

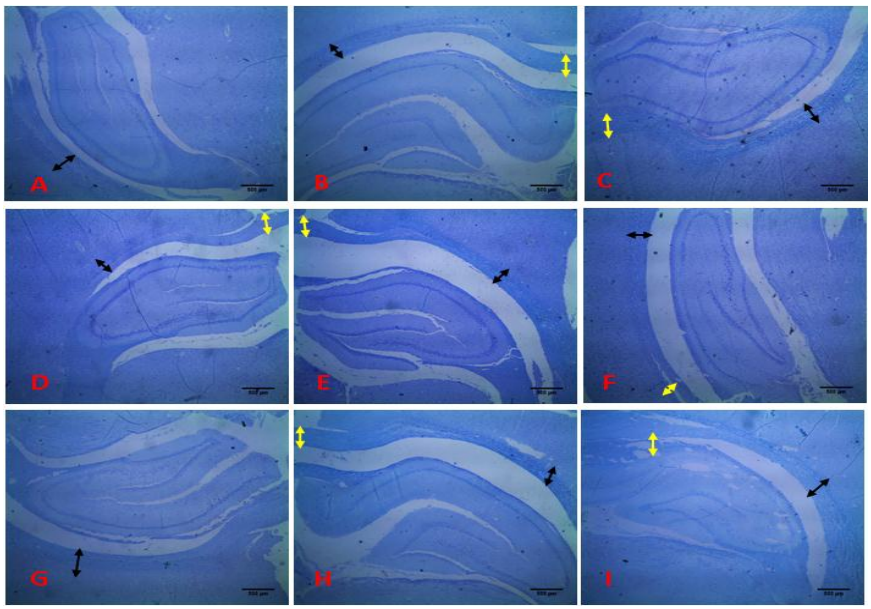

Plate 3.3: Photomicrographs of the hippocampus showing subcortical white matter and corpus callosum subjected to Luxol fast blue stain.

The upper panel represents Acute sub-groups (Control, sham, and experimental A, B, and C respectively), the middle panel represent latent sub-groups (Control, sham, and experimental D, E, and F respectively), the lower panel represents chronic sub-groups (Control, sham and experimental G, H and I respectively). black double head arrow- subcortical white matter, yellow double head arrow- corpus callosum*Hippocampal CA2 subfield was used as the landmark. Scale Bars- 500μm.

DISCUSSION

In this study, the result as shown in (Table 2) there was a significant increase in brain weight in the chronic experimental sub-group, this may be attributed to neuroinflammation which can consequently lead to edema. Neuroinflammation is a consequence of seizures and other neuronal injury events, seizure will cause a release of inflammatory cytokines which may cause brain inflammation and damage the blood-brain barrier. This is in agreement with the work of Marchi *et al.* (2007) who reported that in lithium-pilocarpine induced status epilepticus (SE), pilocarpine causes acute peripheral inflammation mostly through interleukin 1 beta (IL-1β), leading to blood-brain barrier (BBB) leakage and increasing BBB permeability which may promote entry of cofactors into the brain leading to pilocarpine-induced SE. The chronic manifestation of such a feature of inflammation in the study points to the possible progressive nature of blood-brain barrier leakage and permeability. Such progressive pathology could explain why the acute phase did not reveal increased brain weight but the chronic phase did.

This study showed that lithium-pilocarpine administration caused seizures, which resulted in a significant reduction in body weight of all experimental rats during the status epilepticus. In the acute phase, there was a significant reduction in body weight when the experimental sub-group was compared with the control and sham control sub-groups. This reduction in body weight may be attributed to lethargy and reduction in food and water intake secondary to acute seizures. This might suggest that reduction in glucose intake is responsible for the lethargy experienced by the experimental rats and an increased rate in metabolic activity owing to seizure might be responsible for an increase in glucose metabolism. Therefore, glucose utilization plays a key role in status epilepticus. In addition, neuronal excitability and epileptic seizures are directly related to rapid glucose utilization and glycolysis (Schwechter *et al.,* 2003). Seizure has been reported to alter energy balance by reducing food ingestion and increasing energy expenditure (Picard *et al.,* 2000). The latent group also showed a significant reduction in body weight when the experimental sub-group was compared with the control and sham control sub-groups both in acute and latent phases. The increase in body weight points to the fact that the experimental rats started feeding better when seizures stopped, which is the hallmark of the commencement of the latent phase. The better feeding pattern might explain the significant increase in body weight observed in this group. This suggests that epileptogenesis does not affect the feeding center of the brain but hypermetabolism of glucose and lethargy of the acute phase may solely explain the significant reduction in body weight in the acute phase. This trend of body weight change was also observed in the chronic group, the acute phase showed a significant reduction in body weight when the experimental sub-group was compared with the control and sham control sub-groups while the latent phase in the chronic group, also showed a significant decrease in body weight when experimental sub-group was compared with the control and sham sub-groups as also seen in the latent group. This suggests that body weight changes in this group are not a transient occurrence but a sustainable weight loss as seen in the experimental sub-group. The progressive increase in body weight observed across the three phases further affirms the results observed in the acute and latent groups. This suggests that hypremetabolism and lethargy owing to seizures experienced during status epilepticus is the key cause of reduction in body weight loss observed in the experimental sub-groups. Based on the progression of body weight changes observed across the three groups (acute, latent, and chronic) it can be deduced that epileptogenesis in relation to body weight changes is a transient occurrence causing no structural damage to the feeding center (hypothalamus) of the brain but the initial insult (seizure) may be responsible for the acute body weight changes as observed in experimental sub-group of the acute group.

Normal neurons and degenerating neurons were observed in the dorsolateral cerebral cortices of control, sham and experimental sub-groups. The normal neuronal density of control and sham sub-groups was not significantly different when compared with each other across the three groups. This implies that diazepam which is the distinguishing factor between the sham and control sub-groups caused no neuronal degeneration.

In the acute group, there was a significant reduction in the normal neuronal density of the dorsolateral cerebral cortex in the experimental sub-group when compared with control and sham sub-groups. Consequently, there was a significant increase in degenerating neuronal density in the experimental sub-group when compared with control and sham sub-groups. These findings point to the fact that status epilepticus resulted in neuronal injury which presented as evident by acidophilic neurons exhibiting shrunken, condensed, and pyknotic nuclei, eosinophilic neurons with slightly darker nuclei or without identifiable nuclei and karyorrhexis (chromatin fragmentation) as seen in plate 3.1. Previous studies have found neuronal death in the olfactory cortex, amygdaloid complex, thalamus, neocortex, hippocampus and substantia nigra (Turski *et al.,* 1983) in the lithium-pilocarpine model of temporal lobe epilepsy. The extensive neuronal damage as seen in plates 3.2 and 3.3 characterized by shrunken neuronal cell bodies with a

fragmented neuropil appearance was observed in the experimental sub-groups. However, the control and sham sub-groups showed normal neuronal morphology and a non-fragmented neuropil which implies that seizure experienced in the experimental rats not only caused neuronal damage but also resulted in distortion of the neuronal cortical layer and fragmented neuropil. The cortical layers represent horizontal aggregations of neurons with common connections. Therefore, distortion of the cortical layering impedes the normal functional arrangement resulting in disarrangement of neurons normally found in a specified cortical layer.

In the latent group, there was a significant reduction in the normal neuronal density of the dorsolateral cerebral cortex in the experimental sub-group when compared with control and sham sub-groups. However, there was a significant increase in degenerating neuronal density in the experimental sub-group when compared with control and sham sub-groups. The neurodegeneration as seen in plates 3.1 and 3.2, witnessed in the experimental sub-group points to the ongoing epileptogenic events. During the latent phase, several pathophysiological phenomena related to epileptogenesis such as mossy fiber sprouting, interneuron loss, rewiring of synaptic circuits, glial cell activation and ectopic cell proliferation have been reported to be associated with this phase (Dalby and Mody, 2001; Pitk¨anen and Sutula, 2002). The possible mechanism underlying such ongoing epileptogenesis can be explained by biochemical events of epilepsy. Excitatory neurotransmitter (glutamate) is released from presynaptic neurons and acts upon the ionotrophic glutamate receptors Kainate, AMPA (α-Amino-3-hydroxy-5-methyl-4-isoxazolepropionic acid) and NMDA *(*N-Methyl-D-aspartate). Kainate and AMPA receptors cause fast depolarization of neurons by allowing influx of Na+ and K+ and removal of Mg++, whereas NMDA receptors effect a slower depolarization by allowing influx of Ca++ into the post synaptic cell which will induce excitotoxicity and consequently leading to neuronal damage. This study was able to point to neuronal degeneration and increase in oligodendrocyte density as such events showing the ongoing epileptogenesis. The chronic phase follows the latent phase (seizure free phase) and is characterized by the appearance of spontaneous recurrent seizures (SRSs). In this group, as seen in plates 4.2 and 4.3 neuronal degeneration and fragmentation of the neuropil were observed. This might be due to the episodic spontaneous recurrent seizures observed in the experimental sub-group suggesting that in chronic epileptic animals spontaneous seizures could generate changes in neocortical excitability which causes neuronal damage. It has been reported that superficial layers of the sensorimotor cortex are particularly affected with marked atrophy and dendritic sprouting, suggesting lesion, reorganization and neuroplasticity of neocortical networks (Sanabria *et al.,* 2002). Also, the formation of abnormal circuits with synaptic reorganization during epileptogenesis results in changes in neurotransmitter systems which cause an imbalance between excitatory and inhibitory mechanisms consequently leading to spontaneous recurrent seizures which is predominantly seen in the chronic phase. This result corroborates the study of Silva *et al*., (2002) who reported lower normal neuronal density in the chronic epileptic animals. These findings revealed that lithium-pilocarpine-induced TLE causes an increase in the degenerating neuronal density and a decrease in the normal neuronal density of all experimental rats in the three (acute, latent and chronic) groups.

There was a significant increase in number of oligodendrocyte density in the experimental sub-group when compared with control and sham sub-groups across the three groups. The possible explanation might be that oligodendrocyte progenitor cell are known to produce more oligodendrocyte when cell death occurs, progenitor cells had initiated cell proliferation which consequently led to increase in oligodendrocyte density witnessed in the experimental sub-group.

In this study, results revealed a significant increase in the thickness of the subcortical white matter in all experimental sub-groups when compared with the control and sham sub-groups. The increase in thickness might be as a result of looseness or non-compactness of the myelin sheath observed in the experimental groups as against the compact myelin sheath observed in the control and sham sub-groups as seen in plate 3.3. The white matter consists predominantly of myelin sheath and oligodendrocyte. The possible mechanism responsible for myelin sheath damage observed in this study might occur indirectly from neuronal loss or gliosis observed in the dorsolateral cortex of the experimental sub-group. Also, oligodendrocyte injury may occur secondary to the loss of neuron-associated survival support. Once neurons begin to degenerate, the loss of pro-survival signals may affect oligodendrocytes by promoting programmed cell death, as has been shown *in vitro* and during normal development *in vivo* (Barres *et al.,* 1993; Fernandez *et al.,* 2000). Previous studies have shown that oligodendrocytes and their myelin sheaths are more susceptible to damage than other cellular components of the nervous system (Bradl and Lassmann, 2010), Oligodendrocytes can also be damaged as a result of exposure to inflammatory cytokines, such as tumor necrosis factor α (TNFα), which promotes oligodendrocyte cell death by binding to the TNF receptor (Jurewicz *et al.,* 2005). In total, there are many potential mechanisms that may directly contribute to epilepsy-associated oligodendrocyte damage, which, in turn, would contribute to demyelination of the myelin sheath.

The result revealed here was a significant increase in the thickness of the corpus callosum in the experimental sub-group when compared with the control and sham sub-groups of the acute, latent and chronic groups. The corpus callosum presented a wavy appearance in the

experimental sub-groups as seen in plate 4.4. Such wavy appearance of the axonal bundle has been attributed to the commencement of axonal degeneration (Lin *et al.*, 2003). This suggests an apparent loss of myelin integrity substantiating the possible role of epileptogenesis in myelin sheath integrity loss. Such non-compact nature of the corpus callosum and increase in its thickness might be secondary to an edematous state which might be occasioned by the inflammation that normally heralds seizures.

CONCLUSION

In line with the data obtained from this study, the progressive neurodegeneration observed in the cerebral cortex as well as the demylineation dynamics seen in subcortical white matter further explains the scientific basis of epileptogenesis following lithium-pilocarpine-induced TLE.

Funding: This research did not receive any specific grant from funding agencies in the public, commercial, or not-for-profit sectors.

Declaration of interest: None.

Authors' contributions

Ogunsanya Sanmi Tunde: Conception and design, Methodology, Writing – original draft preparation, **Ayannuga Olugbenga Ayodeji**: Conception and design, Supervision, Reviewing and editing, **Owolabi Adegbenga Rolabi**: Supervision, Reviewing and editing, **Osibogun Taiwo Olusola**: Reviewing and editing, **Abijo Ayodeji Zabdiel**: Data analysis. Reviewing and editing. All authors read and approved the final manuscript.

REFERENCES

1. Barkmeier DT, Loeb JA. An animal model to study the clinical significance of interictal spiking. Clin EEG Neurosci, 2009; 40(4): 234–238.
2. Bartolomei F, Khalil M, Wendling F, Sontheimer A, Regis J, Ranjeva JP, et al. Entorhinal behavior and drug action. London: Churchill; 1964. p. 410–8. by intrahippocampal microinjection of pilocarpine. *Epilepsia*, 2002; 4.
3. Bartolomei F, Khalil M, Wendling F, Sontheimer A, Regis J, Ranjeva JP, et al. Entorhinal cortex involvement in human mesial temporal lobe epilepsy: an electrophysiologic and volumetric study. *Epilepsia*, 2005; 46: 677–87.
4. Barres, B., Jacobson, M., Schmid, R., Sendtner, M., Raff, M., Does oligodendrocyte survival depend on axons? *Current. Biology*, 1993; 3: 489.
5. Bertram EH. Temporal lobe epilepsy: where do the seizures really begin? *Epilepsy* Behaviour, 2009; 14(1): 32–37.
6. Bernasconi, N., Bernasconi, A., Andermann, F., Dubeau, F., Feindel, W., Reutens, D.C., Entorhinal cortex in temporal lobe epilepsy: a quantitative MRI study. *Neurology*, 1999; 52: 1870–1876.
7. Bernasconi N., Andermann, F., Arnold, D.L., Bernasconi, A., Entorhinal cortex MRI assessment in temporal, extra temporal, and idiopathic generalized epilepsy. *Epilepsia*, 2003; 44: 1070–1074.
8. Bernasconi N, Duchesne S, Janke A, Lerch J, Collins DL, Bernasconi A. Whole-brainvoxel based statistical analysis of gray matter and white matter in temporal lobe epilepsy. *Neuroimage*, 2004; 23: 717-723.
9. Bernhardt B.C., Worsley, K.J., Besson, P., Concha, L., Lerch, J.P., Evans, A.C., et al., Mapping limbic network organization in temporal lobe epilepsy using morphometric correlations: insights on the relation between mesiotemporal connectivity and corti- cal atrophy. *NeuroImage*, 2008; 42(2): 515–524.
10. Bernhardt BC, Worsley KJ, Kim H, Evans AC, Bernasconi A, Bernasconi N. Longitudinal and cross section alanalysis of atrophy in pharmacoresistant temporal lobe epilepsy. *Neurology*, 2009; 72: 1747-1754.
11. Bernhardt BC, Bernasconi N, Concha L, Bernasconi A. Cortical thickness analysis in temporal lobe epilepsy: reproducibility and relation to outcome.*Neurology*, 2010; 74: 1776-1784.
12. Bjartmar C., Hildebrand C., Loinder K., Morphological heterogeneity of rat oligodendrocytes: electronmicroscopic studies on serial sections. Glia, 1994; 11: 235.
13. Borges K, Gearing M, McDermott DL, Smith AB, Almonte AG, Wainer BH, Dingledine R. Neuronal and glial pathological changes during epileptogenesis in the mouse pilocarpine model. *Experimental Neurology*, 2003; 182: 21–34.
14. Boss BD, Peterson GM, Cowan WM. On the number of neurons in the dentate gyrus of the rat. Brain Res., 1985; 338: 144-50.
15. Bradl M., Lassmann, H., Oligodendrocytes: biology and pathology. Act a *Neuropathology*, 2010; 119: 37–53.
16. Brown T H, Zador AM. Hippocampus. In: The synaptic organization of the brain, Shepherd G.M. ed. Oxford, 2008; 346-388.
17. Berges S, Seizures and epilepsy following strokes: recurrence factors. *European journal of Neurology*, 2000; 43(1): 3-8.
18. Brown P, and Thompson P.D., Rothwell J. C., Day B. L. and Marsden C. D.; Axial myoclonus of propriospinal origin. *Brain*, 1991; 114: 197-214.
19. Cascino GD. Temporal lobe epilepsy is a progressive neurologic disorder: time means neurons. *Neurology*, 2009; 72: 1718-1719.
20. Claiborne BJ, Amaral DG, Cowan WM. A light and electron microscopic analysis of the mossy fibers of the rat dentate gyrus. *Journal of Computerized Neurology*, 1986; *246:* 435-58.
21. Coan AC, Appenzeller S, Bonilha L, Li LM, Cendes F. Seizure frequency and lateralization affect

progression of atrophy in temporal lobe epilepsy. *Neurology*, 2009; 73: 834-842.
22. Cockerell O. C. The mortality of epilepsy; *Current Opinion Neurology*, 1996; 9(2): 93-96.
23. Concha L, Beaulieu C, Gross DW. Bilateral limbic diffusion abnormalities in unilateral temporal lobe epilepsy. *AnnNeurology*, 2005; 57: 188-196.
24. Cook, L.L., Persinger, M.A., Demands during maze learning in limbic epileptic rats: selective damage in the thalamus Perception Motor Skills, 1996; 83: 323–329.
25. Coste, S., Ryvlin, P., Hermier, M., Ostrowsky, K., Adeleine, P., From ent, J.C., Mauguiere, F., Temporopolar changes in temporal lobe epilepsy: a quantitative MRI-based study. *Neurology*, 2002; 59: 855–861.
26. Fisher RS, van Emde Boas W, Blume W, Elger C, Genton P, Lee P, et al. Epileptic seizures and epilepsy: definitions proposed by the International League Against Epilepsy (ILAE) and the International Bureau for Epilepsy (IBE). *Epilepsia*, 2005; 46: 470–2.